Rare Metal Materials and Engineering
Volume 50, Issue 10, October 2021
Available online at www.rmme.ac.cn

Science Press

Cite this article as: Ju Jiantao, Zhu Zhihong, Yang Kangshuai, et al. Control of Al and Ti Contents During Electroslag Remelting of High-Temperature Ni-based Alloys[J]. Rare Metal Materials and Engineering, 2021, 50(10): 3550-3561.

REVIEW

Control of Al and Ti Contents During Electroslag Remelting of High-Temperature Ni-based Alloys

Ju Jiantao[1,2], Zhu Zhihong[1,2], Yang Kangshuai[1,2], Ji Guangheng[1,2], An Jialiang[1,2], Shi Cheng-bin[3]

[1] School of Metallurgical Engineering, Xi'an University of Architecture and Technology, Xi'an 710055, China; [2] Metallurgical Engineering Technology Research Centre of Shaanxi Province, Xi'an 710055, China; [3] State Key Laboratory of Advanced Metallurgy, University of Science and Technology Beijing, Beijing 100083, China

Abstract: The oxidation of Al and Ti in the electroslag remelting process causes an uneven axial composition of the electroslag ingot, which adversely affects its performance, including corrosion resistance and mechanical properties. To control the uniformity of Al and Ti content in electroslag ingots, it is necessary to clarify the change in Al and Ti content during the high-temperature electroslag remelting and to reduce the oxidation of Al and Ti in the alloy by optimizing the slag system ratio and smelting conditions. The research status of Al and Ti element control in the electroslag remelting process was reviewed based on the existing literature, taking the low-fluorine slag CaF_2-CaO-Al_2O_3-MgO-TiO_2 and Incoloy 825 alloy as examples. The ion and molecular coexistence theory of slag (IMCT) was used along with FactSage software to summarize the thermodynamic and kinetic research methods. The effects of temperature and components of slag on the equilibrium Al and Ti contents in the alloy were discussed. Based on the film-penetration theory, a kinetics model for predicting Al and Ti contents in the alloy was proposed, and the mathematical equation of the Al and Ti contents vs time in the electroslag process and the slag-metal reaction rate-limiting method were obtained. Results show that the optimum TiO_2 addition during the electroslag remelting for Incoloy 825 alloy is determined to be approximately 10%. The slag-metal equilibrium experimental results were compared and analyzed using IMCT and FactSage. It is found that the FactSage calculation results are more accurate than the IMCT calculation results. The higher the TiO_2 content, the smaller the deviation between the calculated and experimental results.

Key words: electroslag remelting; Al, Ti content; thermodynamics; IMCT; kinetics

Alloys and steels refined by electroslag remelting are commonly used in aerospace and petrochemical fields[1], so there are strict requirements on all aspects of their performance, and the alloying elements Al and Ti in the metal are the key elements that determine their performance. For example, the high-temperature nickel-based alloys are solid solution-strengthened Fe-Cr-Ni-based corrosion-resistant alloys. The Al and Ti contents in the alloy determine the strengthening phase γ'-Ni_3(Al, Ti), the precipitation temperature, and the amount of Ti(C, N), which in turn affect the alloy's structure, mechanics, corrosion resistance, and melting point of the alloy[2-4]. At present, the main production methods for most high-temperature nickel-based alloys are vacuum melting and electroslag remelting. However, the oxidation-reduction reaction between the slag and the metal during the electroslag remelting process causes the metal elements Al and Ti in the electroslag ingot to be oxidized. This results in their uneven distribution in the axial direction, and seriously affects the quality of the electroslag ingot[5-8].

Current research methods of component content control in the electroslag process rely upon theoretical calculations combined with experimental verification. Researchers have proposed a large number of reaction models, including thermodynamic models, kinetic models, deoxidation models, and desulphurisation models, to predict the content changes of various components[9-13]. The study of the control of Al and Ti

Received date: March 03, 2021
Foundation item: National Natural Science Foundation of China (51774225)
Corresponding author: Ju Jiantao, Ph. D., Professor, School of Metallurgical Engineering, Xi'an University of Architecture and Technology, Xi'an 710055, P. R. China, Tel: 0086-29-82205114, E-mail: jujiantao_0033@163.com

content employs mainly a thermodynamic model and a kinetic model. In the case of an argon atmosphere or addition of a deoxidizer, the oxidation reaction equation of Al and Ti in the alloy is as follows[14,15]:

$$4[Al]+3(TiO_2)=3[Ti]+2(Al_2O_3) \quad (1)$$

The Al_2O_3 content in the slag is high, and the Ti content in the high-titanium and low-aluminium alloy is much higher than the Al content, which causes the Ti element to be easily oxidized. At present, the focus of thermodynamics research is to determine the optimal amount of TiO_2 in the slag when the content of Al and Ti in the alloy is controlled. However, the TiO_2 content required for smelting is not only related to the type of alloy but also affected by the content of other components in the slag. For different alloys, the optimal TiO_2 content in the slag is variable. The focus of kinetics research is to predict the distribution of Al and Ti elements in electroslag ingots based on actual electroslag process parameters and slag composition[16-18]. This more closely represents actual conditions. The influence of slag composition and smelting conditions on Al and Ti content can be determined, and the formulation of process parameters in the electroslag process can be clarified. Therefore, it is important to summarize the previous research methods and results to obtain the change regularity and mechanism of Al and Ti content during the electroslag remelting process.

This paper summarizes the research progress on the control of Al and Ti content during the electroslag remelting process. In addition, based on the ion and molecular coexistence theory of slag (IMCT) and FactSage (GTT-Technologies, DE) software calculations, the changes in the equilibrium Al and Ti contents of the CaF_2-CaO-Al_2O_3-MgO-TiO_2 slag reaction with Incoloy 825 alloy were identified. The oxidation regularity of Al and Ti during the electroslag remelting of the Incoloy 825 alloy reveals the optimal TiO_2 content in the slag. To provide theoretical guidance for the control of Al and Ti content in the process of electroslag remelting, a kinetic model for predicting Al and Ti contents was proposed based on the film permeation theory.

1 Thermodynamic Calculation Method

The thermodynamic calculation of Al and Ti contents during the electroslag remelting process can provide theoretical support for the slag system design, and the key in the calculation is the component activity in the slag. The reaction of Al and Ti vs Al_2O_3 and TiO_2 in the slag during the electroslag remelting process under the protection of argon has been shown in Eq.(1), and the equilibrium constant of the reaction is shown in Eq.(2)[19]:

$$\lg K = \lg \frac{a_{Ti}^3 \cdot a_{Al_2O_3}^2}{a_{Al}^4 \cdot a_{TiO_2}^3} = \lg \frac{f_{Ti}^3[Ti]}{f_{Al}^4[Al]} + \lg \frac{a_{Al_2O_3}^2}{a_{TiO_2}^3} = \frac{35300}{T} - 9.94 \quad (2)$$

where a_{Al} and a_{Ti} are the activities of Al and Ti in the alloy, and a_{TiO_2} and $a_{Al_2O_3}$ are the activities of TiO_2 and Al_2O_3 in the slag, respectively; the coefficients f_{Al} and f_{Ti} are the activity coefficients of Al and Ti elements, respectively, and are calculated using Wagner's equation in the alloy with 1% as the standard state, as shown in Eq.(3):

$$\lg f_i = \sum e_i^j[\%j] \quad (3)$$

where f_i represents the activity coefficient of element i in the alloy; e_i^j represents the activity interaction coefficient of element j with respect to element i in the alloy. The activity interaction coefficients of the components in the alloy are listed in Table 1. The Incoloy 825 alloy composition is shown in Table 2.

1.1 IMCT calculation of component activity in slag

According to the theoretical assumption of IMCT, the structural units existing in the slag system include four simple ions of Ca^{2+}, Mg^{2+}, F^-, and O^{2-}, two simple molecules of Al_2O_3 and TiO_2 [24,25], other related compounds (Table 3), and related chemical reactions (Table 4). The mole fraction of oxide in the slag can be expressed as $b_1 = n_{CaO}^0$, $b_2 = n_{CaF_2}^0$, $b_3 = n_{MgO}^0$, $b_4 = n_{Al_2O_3}^0$, $b_5 = n_{TiO_2}^0$. According to the definition of IMCT, Eq.(4~9) can be acquired by defining N_1, N_2, N_3, N_4, and N_5 as the active concentrations of the components. MATLAB R2017b (MathWorks, USA) was used to perform the calculations based on Eq.(4~9).

$$N_1 + N_2 + \cdots + N_5 + N_{c1} + N_{c2} + \cdots + N_{c15} = \sum N_i = 1 \quad (4)$$

$$b_1 = (0.5N_1 + N_{c1} + 3N_{c3} + 12N_{c4} + N_{c5} + N_{c6} + N_{c7} + 3N_{c8} + 4N_{c9} + 3N_{c14} + 11N_{c15})\sum n_i = n_{CaO}^0 \quad (5)$$

$$b_2 = (1/3N_2 + N_{c15} + N_{c16})\sum n_i = n_{CaF_2}^0 \quad (6)$$

$$b_3 = (0.5N_3 + N_{c2} + N_{c11} + N_{c12} + 2N_{c13})\sum n_i = n_{MgO}^0 \quad (7)$$

$$b_4 = (N_4 + N_{c1} + N_{c2} + N_{c3} + 7N_{c4} + 2N_{c5} + 6N_{c6} + N_{c10} + N_{c14} + 3N_{c15} + 7N_{c16})\sum n_i = n_{Al_2O_3}^0 \quad (8)$$

$$b_5 = (N_5 + N_{c7} + 2N_{c8} + 3N_{c9} + N_{c10} + N_{c11} + 2N_{c12} + N_{c13})\sum n_i = n_{TiO_2}^0 \quad (9)$$

1.2 FactSage calculation of component activity in slag

FactSage 7.3 thermodynamic software was used to calculate the Al_2O_3 and TiO_2 activities in the slag at 1773 K. The FactPS and FToxid databases were used in the software. The pure solid standard state was selected for the calculation results.

Table 1 Activity interaction coefficient e_i^j of the alloying elements in Incoloy 825 alloy[20-23]

Element	Mn	Cr	Ni	Al	Ti	Cu	Mo
Al	0.034	0.045	-0.0376	0.040	-	-	-
Ti	-0.120	0.025	-0.0166	-	0.048	0.014	0.016

Table 2 Chemical composition of the Incoloy 825 alloy (wt%)

C	Mn	Si	P	S	Cr	Mo	Ni	Cu	Al	Ti	O	Fe
0.010	0.107	0.131	0.009	0.009	20.620	3.180	38.880	1.660	0.120	1.000	0.0026	Bal.

Table 3 Expression of structural units as ion couples or complex molecules, their mole numbers, and mass action concentrations in 100 g CaF_2-CaO-Al_2O_3-MgO-TiO_2 slags based on IMCT

Item	Structural units as ion couples or molecules	Number of structural units or ion couples	Mole number of structural unit, n_i/mol	Mass action concentration of structural unit or ion couple, N_i
Simple cation	$Ca^{2+}+O^{2-}$	1	$n_1 = n_{Ca^{2+},CaO} = n_{O^{2-},CaO}$	$N_1 = \frac{2n_1}{\sum n_i} = N_{CaO}$
	$Ca^{2+}+2F^{2-}$	2	$n_2 = n_{Ca^{2+},CaF_2} = 2n_{F^-,CaF_2}$	$N_2 = \frac{3n_2}{\sum n_i} = N_{CaF_2}$
	$Mg^{2+}+O^{2-}$	3	$n_3 = n_{Mg^{2+},MgO} = n_{O^{2-},MgO}$	$N_3 = \frac{2n_3}{\sum n_i} = N_{MgO}$
Simple molecule	Al_2O_3	4	$n_4 = n_{Al_2O_3}$	$N_4 = \frac{n_4}{\sum n_i} = N_{Al_2O_3}$
	TiO_2	5	$n_5 = n_{TiO_2}$	$N_5 = \frac{n_5}{\sum n_i} = N_{TiO_2}$
Complex molecule	$CaO\cdot Al_2O_3$	$c1$	$n_{c1} = n_{CaO\cdot Al_2O_3}$	$N_{c1} = \frac{n_{c1}}{\sum n_i} = N_{CaO\cdot Al_2O_3}$
	$MgO\cdot Al_2O_3$	$c2$	$n_{c2} = n_{MgO\cdot Al_2O_3}$	$N_{c2} = \frac{n_{c2}}{\sum n_i} = N_{MgO\cdot Al_2O_3}$
	$3CaO\cdot Al_2O_3$	$c3$	$n_{c3} = n_{3CaO\cdot Al_2O_3}$	$N_{c3} = \frac{n_{c3}}{\sum n_i} = N_{3CaO\cdot Al_2O_3}$
	$12CaO\cdot 7Al_2O_3$	$c4$	$n_{c4} = n_{12CaO\cdot 7Al_2O_3}$	$N_{c4} = \frac{n_{c4}}{\sum n_i} = N_{12CaO\cdot 7Al_2O_3}$
	$CaO\cdot 2Al_2O_3$	$c5$	$n_{c5} = n_{CaO\cdot 2Al_2O_3}$	$N_{c5} = \frac{n_{c5}}{\sum n_i} = N_{CaO\cdot 2Al_2O_3}$
	$CaO\cdot 6Al_2O_3$	$c6$	$n_{c6} = n_{CaO\cdot 6Al_2O_3}$	$N_{c6} = \frac{n_{c6}}{\sum n_i} = N_{CaO\cdot 6Al_2O_3}$
	$CaO\cdot TiO_2$	$c7$	$n_{c7} = n_{CaO\cdot TiO_2}$	$N_{c7} = \frac{n_{c7}}{\sum n_i} = N_{CaO\cdot TiO_2}$
	$3CaO\cdot 2TiO_2$	$c8$	$n_{c8} = n_{3CaO\cdot 2TiO_2}$	$N_{c8} = \frac{n_{c8}}{\sum n_i} = N_{3CaO\cdot 2TiO_2}$
	$4CaO\cdot 3TiO_2$	$c9$	$n_{c9} = n_{4CaO\cdot 3TiO_2}$	$N_{c9} = \frac{n_{c9}}{\sum n_i} = N_{4CaO\cdot 3TiO_2}$
	$Al_2O_3\cdot TiO_2$	$c10$	$n_{c10} = n_{Al_2O_3\cdot TiO_2}$	$N_{c10} = \frac{n_{c10}}{\sum n_i} = N_{Al_2O_3\cdot TiO_2}$
	$MgO\cdot TiO_2$	$c11$	$n_{c11} = n_{MgO\cdot TiO_2}$	$N_{c11} = \frac{n_{c11}}{\sum n_i} = N_{MgO\cdot TiO_2}$
	$MgO\cdot 2TiO_2$	$c12$	$n_{c12} = n_{MgO\cdot 2TiO_2}$	$N_{c12} = \frac{n_{c12}}{\sum n_i} = N_{MgO\cdot 2TiO_2}$
	$2MgO\cdot TiO_2$	$c13$	$n_{c13} = n_{2MgO\cdot TiO_2}$	$N_{c13} = \frac{n_{c13}}{\sum n_i} = N_{2MgO\cdot TiO_2}$
	$3CaO\cdot 3Al_2O_3\cdot CaF_2$	$c14$	$n_{c14} = n_{3CaO\cdot 3Al_2O_3\cdot CaF_2}$	$N_{c14} = \frac{n_{c14}}{\sum n_i} = N_{3CaO\cdot 3Al_2O_3\cdot CaF_2}$
	$11CaO\cdot 7Al_2O_3\cdot CaF_2$	$c15$	$n_{c15} = n_{11CaO\cdot 7Al_2O_3\cdot CaF_2}$	$N_{c15} = \frac{n_{c15}}{\sum n_i} = N_{11CaO\cdot 7Al_2O_3\cdot CaF_2}$

The expressions of the equilibrium Al and Ti contents in the alloy are shown in Eq.(10) and Eq.(11), respectively:

$$\lg X'_{Ti} = \frac{1}{3}\left(\begin{array}{l}\lg\dfrac{a^3_{TiO_2}}{a^2_{Al_2O_3}} + 4\lg f_{Al} + 4\lg X_{Al} \\ -3\lg f_{Ti} + \dfrac{35300}{T} - 9.94\end{array}\right) \quad (10)$$

$$\lg X'_{Al} = \frac{1}{4}\left(\begin{array}{l}\lg\dfrac{a^2_{Al_2O_3}}{a^3_{TiO_2}} - 4\lg f_{Al} + 3\lg X_{Ti} \\ +3\lg f_{Ti} - \dfrac{35300}{T} + 9.94\end{array}\right) \quad (11)$$

where X_{Ti} and X_{Al} are the initial Ti and Al contents in the alloy, and X'_{Ti} and X'_{Al} are the equilibrium Ti and Al contents in the

Table 4 Chemical reaction formulas of possibly formed complex molecules[26-28]

Reaction	ΔG_i^θ/J·mol^{-1}	N_i
$(Ca^{2+}+O^{2-}) + (Al_2O_3) = (CaO\cdot Al_2O_3)$	$59413 - 59.413T$	$N_{c1} = K_{c1}N_1N_4$
$(Mg^{2+} + O^{2-}) + (Al_2O_3) = (MgO\cdot Al_2O_3)$	$-18828 - 6.276T$	$N_{c2} = K_{c2}N_3N_4$
$3(Ca^{2+} + O^{2-}) + (Al_2O_3) = (3CaO\cdot Al_2O_3)$	$-21757 - 29.288T$	$N_{c3} = K_{c3}N_1^3N_4$
$12(Ca^{2+} + O^{2-}) + 7(Al_2O_3) = (12CaO\cdot 7Al_2O_3)$	$617977 - 612.119T$	$N_{c4} = K_{c4}N_1^{12}N_4^7$
$(Ca^{2+} + O^{2-}) + 2(Al_2O_3) = (CaO\cdot 2Al_2O_3)$	$-16736 - 25.522T$	$N_{c5} = K_{c5}N_1N_4^2$
$(Ca^{2+} + O^{2-}) + 6(Al_2O_3) = (CaO\cdot 6Al_2O_3)$	$-22594 - 31.798T$	$N_{c6} = K_{c6}N_1N_4^6$
$(Ca^{2+} + O^{2-}) + (TiO_2) = (CaO\cdot TiO_2)$	$-79900 - 3.35T$	$N_{c7} = K_{c7}N_1N_5$
$3(Ca^{2+} + O^{2-}) + 2(TiO^2) = (3CaO\cdot 2TiO_2)$	$-207100 - 11.35T$	$N_{c8} = K_{c8}N_1^3N_5^2$
$4(Ca^{2+} + O^{2-}) + 3(TiO^2) = (4CaO\cdot 3TiO_2)$	$-292880 - 17.573T$	$N_{c9} = K_{c9}N_1^4N_5^3$
$(Al_2O_3) + (TiO_2) = (Al_2O_3\cdot TiO_2)$	$-25270 + 3.924T$	$N_{c10} = K_{c10}N_4N_5$
$(Mg^{2+} + O^{2-}) + (TiO_2) = (MgO\cdot TiO_2)$	$-26400 + 3.14T$	$N_{c11} = K_{c11}N_3N_5$
$(Mg^{2+} + O^{2-}) + 2(TiO_2) = (MgO\cdot 2TiO_2)$	$-27600 + 0.63T$	$N_{c12} = K_{c12}N_3N_5^2$
$2(Mg^{2+} + O^{2-}) + (TiO_2) = (2MgO\cdot TiO_2)$	$-25500 + 1.26T$	$N_{c13} = K_{c13}N_3^2N_5$
$3(Ca^{2+}+ O^{2-}) + 3(Al_2O_3) + (Ca^{2+} + 2F^-) = (3CaO\cdot 3Al_2O_3\cdot CaF_2)$	$-44492 - 73.15T$	$N_{c14} = K_{c14}N_1^3N_2N_4^3$
$11(Ca^{2+}+ O^{2-}) + 7(Al_2O_3) + (Ca^{2+}+2F^-) = (11CaO\cdot 7Al_2O_3\cdot CaF_2)$	$-228760 - 155.8T$	$N_{c15} = K_{c15}N_1^{11}N_2N_4^7$

alloy, respectively.

2 Oxidation Regularity of Al and Ti Content in Alloy

A thermodynamic study of the electroslag remelting process can obtain the equilibrium Al and Ti content in the alloy at the end of the slag-metal reaction under the condition that the alloy and slag compositions are fixed. It is usually used to determine the optimal amount of TiO_2 in the slag to provide a theoretical basis for further research. Pateisky et al[19] used different slags for electroslag remelting experiments, and the changes in Al, Ti, and Si contents during the electroslag remelting process were studied. It was found that the reaction of Ti and Si in steel with Al_2O_3 in slag does not cause a uniform distribution of axial components in the ingot. Appropriate addition of TiO_2 and SiO_2 to the slag can reduce the loss of Ti and Si. Duan et al[29] systematically studied the effects of components and temperature of the slag on the equilibrium Al and Ti content in the alloy with the help of IMCT, and summarized the effects of the slag components on the oxidation behavior of Al and Ti elements in the alloy. The calculation result of equilibrium Ti content and component of slag is shown in Fig. 1. And the relative importance of factors controlling the oxidation of Al and Ti is in the following order: TiO_2>Al_2O_3>CaO>CaF_2>MgO. It can be observed that as the temperature increases, the equilibrium Ti content gradually decreases. At the same time, the kinetic model proves that the mass transfer rate of Al and Ti in the alloy is much greater than that of Al_2O_3 and TiO_2 in the slag. Hou et al[30] proposed a thermodynamic model for the deoxidation of 1Cr21Ni5Ti stainless steel during electroslag remelting. When the amount of Al added is 0.15%, and the amount of TiO_2 added to the slag is 4wt%, the Ti element of the steel can be ensured not to lose.

According to Eq. (10) and Eq. (11), the relationship of the equilibrium Ti and Al content in the alloy with the component content in the slag at different temperatures as calculated by both IMCT and FactSage is shown in Fig. 2 and Fig. 3, respectively. As the temperature increases from 1773 K to 1973 K, the oxidation of Ti in the alloy increases. The main reason is that as the temperature increases, the Gibbs free energy of Eq. (1) increases continuously, and the tendency of the reaction to proceed in the reverse direction increases. Yang and Park et al[31] studied the slag-metal equilibrium experiment of CaF_2-CaO-Al_2O_3-TiO_2 and Ni-based alloys from 1773 K to 1873 K, and calculated the activity-composition relationship of Al_2O_3 and TiO_2 in slag from 1823 K to 1873 K using FactSage software. The relationship is shown in Fig. 4. Fig. 4a indicates that when the activity ratio of Al_2O_3 and TiO_2 is constant, the higher the temperature, the larger the ratio of Al_2O_3 to TiO_2. More TiO_2 is then needed to prevent Ti loss.

From Fig. 2a, 2b, 3a and 3b, it can be observed that as the slag increases (0% to 35%), the equilibrium Ti content in the alloy decreases significantly, and the Al content increases significantly. When the content of Al or CaO is less than 15%, the degree of influence is Al_2O_3>CaO, but the loss of the equilibrium Ti content in the alloy is significantly slowed as the content of Al_2O_3 increases to larger than 15wt%. This is because as the Al_2O_3 content increases to 15wt%, the reaction between Al_2O_3 and CaO is strengthened, the activity of Al_2O_3 in the slag decreases, and the reaction strength of Al_2O_3 and Ti in the alloy is reduced, causing a decrease in the Ti content. Jiang et al[32] proved that CaO can promote the oxidation of Ti in GH8825 alloy through experiments and calculations of CaF_2-CaO-Al_2O_3-MgO-TiO_2-SiO_2 slag and GH8825 alloy slag at 1823 K. As shown in Fig. 5a, as the CaO content increases, the Ti is oxidized and the Al content is increased. The main reason is that the optical basicity of TiO_2 is smaller than that of Al_2O_3, and CaO is more easily combined with TiO_2. With the increase in CaO content, the activity of TiO_2 evidently decreases. Hou et al[33] reported that the increase in CaO

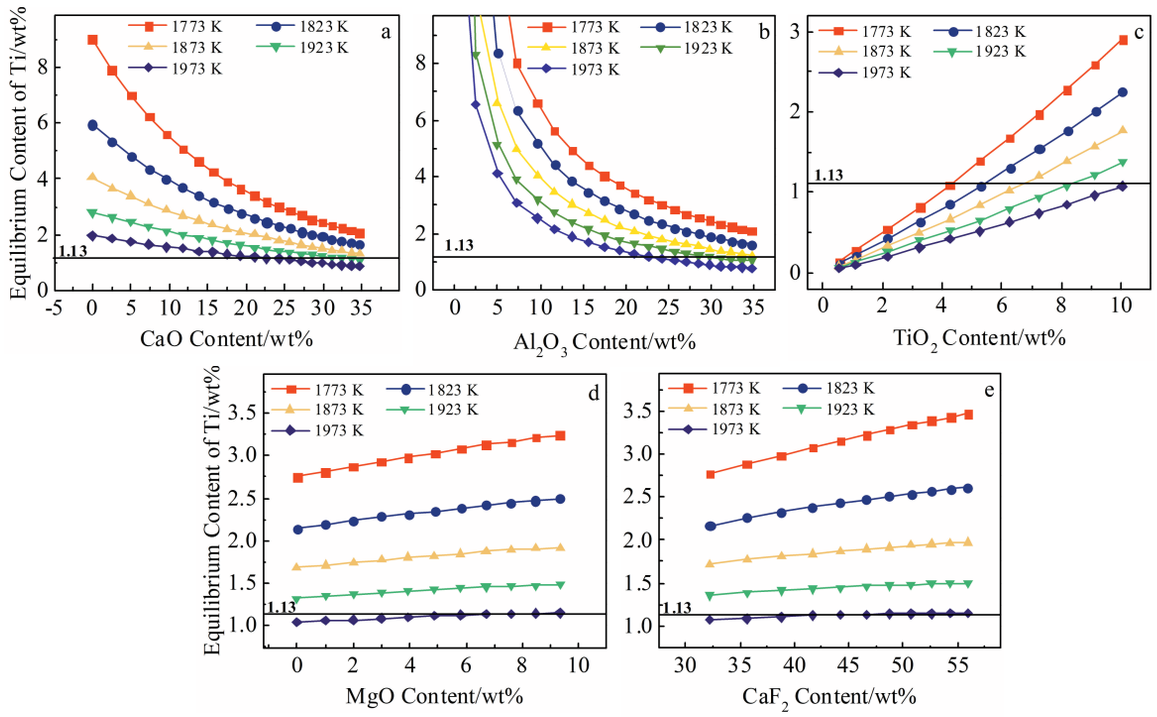

Fig.1 Calculation result of relationship between equilibrium Ti and component of slag[29]: (a) CaO, (b) Al_2O_3, (c) TiO_2, (d) MgO, and (e) CaF_2

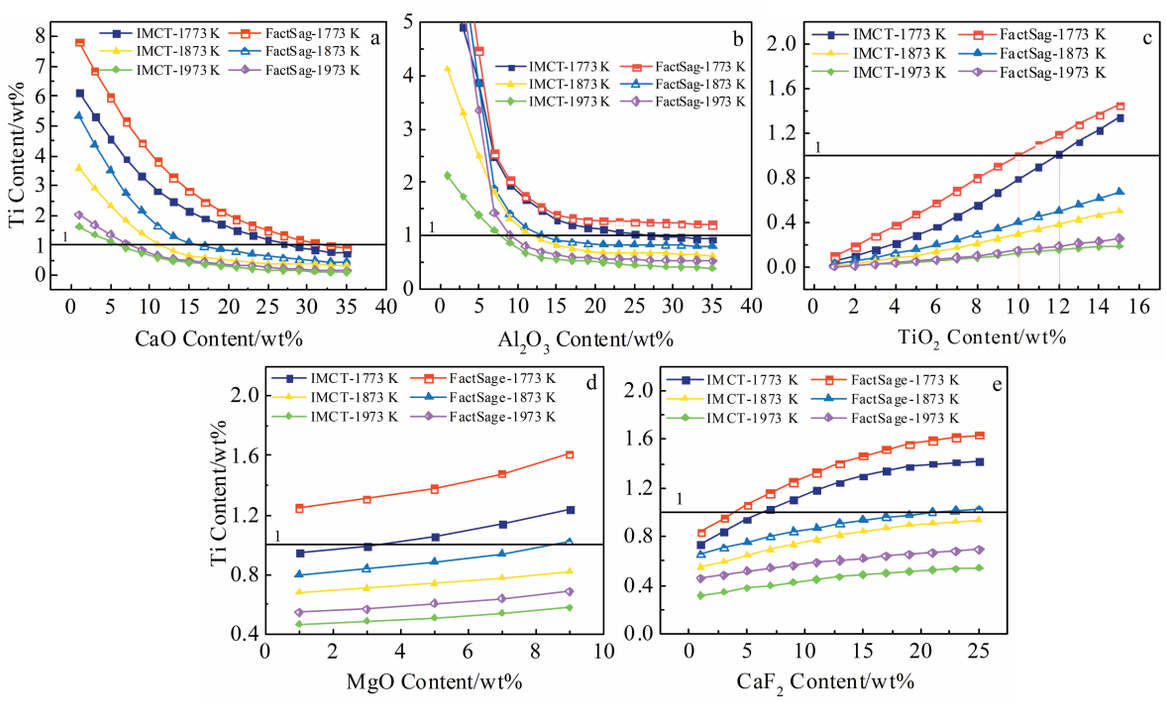

Fig.2 Relationship between component content in slag and equilibrium Ti content in alloy: (a) CaO, (b) Al_2O_3, (c) TiO_2, (d) MgO, and (e) CaF_2

content during the reaction of CaF_2-Al_2O_3-CaO-MgO-TiO_2-SiO_2 slag with 1Cr21Ni5Ti stainless steel significantly inhibits Al oxidation in the alloy and intensifies Ti oxidation. Therefore, when the content of CaO in the slag is high, it is necessary to increase the content of TiO_2 to inhibit the oxidation of Ti in the alloy. This is especially true for low-fluorine slag, where the content of CaO and Al_2O_3 in the slag is higher, and control of the Ti element requires more TiO_2 in the slag. At the same time, the relationship between Al_2O_3 and TiO_2 in the slag and the content of Al and Ti in the steel under

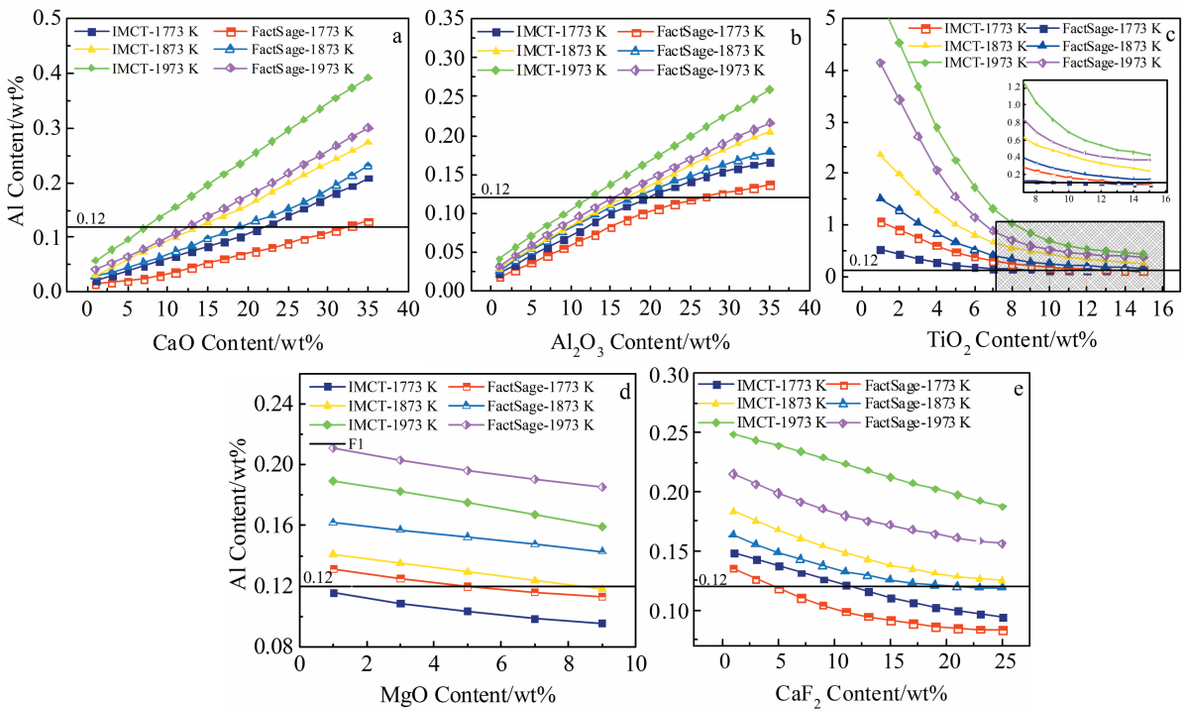

Fig.3 Relationship between composition of slag and equilibrium Al content in alloy: (a) CaO, (b) Al_2O_3, (c) TiO_2, (d) MgO, and (e) CaF_2

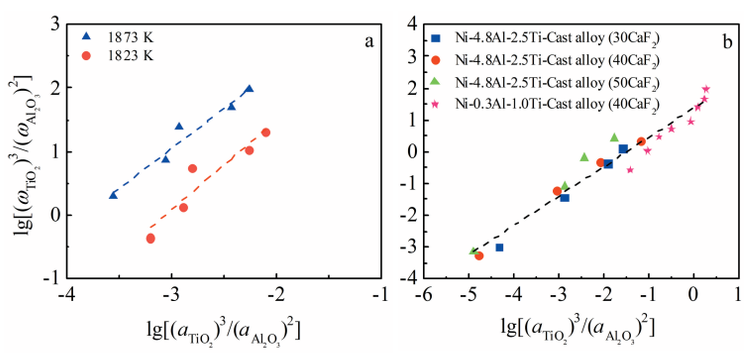

Fig.4 Activity-composition relationship of Al_2O_3 and TiO_2 in slag[31]: (a) different temperatures and (b) different CaF_2 contents

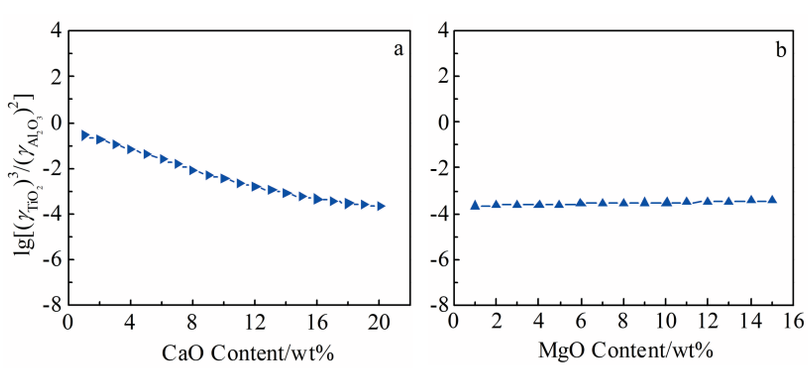

Fig.5 Effect of CaO and MgO on lg $[(\gamma_{TiO_2})^3/(\gamma_{Al_2O_3})^2]$ in slag[32]: (a) CaO and (b) MgO

different temperatures and CaO contents is established. Fig. 6 shows that the contents of Al and Ti remain unchanged and they are the corresponding components of the slag.

From Fig. 2c~2e and Fig. 3c~3e, one can see that as the

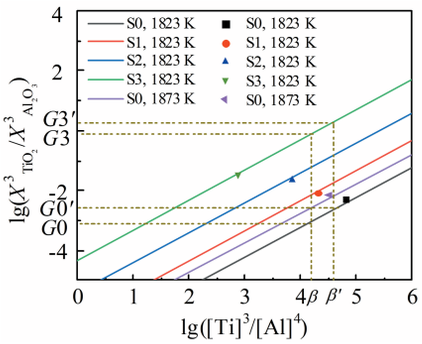

Fig.6 Relationship between Al/Ti in steel and Al_2O_3/TiO_2 in slag[33]

content of TiO_2, CaF_2, and MgO in the slag increases, the content of Ti in the alloy increases, and the content of Al decreases. The relative magnitudes of their effects are TiO_2> CaF_2>MgO. Increasing the TiO_2 content can significantly inhibit the loss of Ti in the alloy. This is due to the increased reactivity of the TiO_2 content with Al in the alloy. The Al in the alloy is oxidized to Al_2O_3 in the slag, and the Ti is reduced in the alloy. However, the initial Al and Ti contents in different alloys differ, and the optimal TiO_2 addition also differs. Duan et al[34] showed that during the reaction of the CaF_2-Al_2O_3-CaO-MgO-TiO_2 slag system and the Inconel 718 alloy (Al and Ti contents are 0.43wt% and 1.13wt% , respectively) at 1773 K, the optimal TiO_2 content in the slag is 4wt% . The results are shown in Fig. 7. The optimal TiO_2 addition for smelting the Incoloy 825 alloy at 1773 K is shown in Fig. 2c. The calculated result using IMCT is 10%, and the calculated result using FactSage7.1 is 12%. Compared with the Inconel 718 alloy, the optimal content of TiO_2 for the Incoloy 825 alloy is higher. Because the contents of Al and Ti in the alloy differ greatly, more TiO_2 is required to control the loss of Ti in the alloy. Moreover, the appropriate addition of TiO_2 to the slag can not only control the loss of Ti in the alloy, but also reduce the viscosity of the slag[35], which is beneficial for optimizing the kinetic conditions of the slag-metal reaction. From the calculation results of Jiang et al[32] highlighted in Fig. 5b, it can be observed that the value of

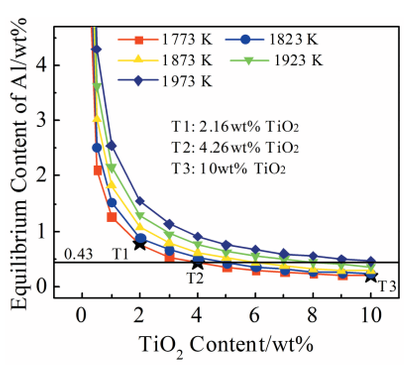

Fig.7 Relationship between equilibrium Al and Ti contents in the alloy and TiO_2 contents in the slag using IMCT[34]

lg [$(\gamma_{TiO_2})^3/(\gamma_{Al_2O_3})^2$] changes with the increase in MgO content is very small (γ_{iO_x} represents the activity coefficient of component in slag). This shows that the change in MgO content has little effect on the equilibrium Al and Ti content in the alloy. From the experimental results of Yang and Park[31] in Fig. 4b, we can see that the effect of CaF_2 content on the changes in Al and Ti content in the alloy is small. The CaF_2 content improves the fluidity and conductivity of the slag.

Comparing the calculated results of IMCT with those of FactSage in Fig. 2 and Fig. 3, it is observed that the oxidation of Ti in the alloy is greater than that obtained using FactSage. As can be seen from Fig. 2c and Fig. 3c, the FactSage results show that the optimal TiO_2 content for controlling Al and Ti content in the alloy at 1773 K is 10%, while the IMCT calculation results show that it is 12%. The higher calculated result of IMCT indicates that the Ti element in the alloy has excessive loss when calculated by IMCT. In a previous study, the author conducted a high-temperature slag-metal equilibrium experiment on CaF_2-CaO-Al_2O_3-MgO-Li_2O-TiO_2 low-fluorine slag and Incoloy 825 alloy at 1773 K[36]. The experimental results are shown in Fig. 8. The deviation between the calculated results of FactSage/IMCT and the experimental result is shown in Fig. 9. It can be observed that the calculated result of FactSage has small deviation from the experimental result, while the calculated result of IMCT has a slightly larger deviation from the experimental result. There are two reasons for this result. First, loop iteration method in MATLAB is used in the IMCT calculation process, and certain errors occur during the process. Second, the FactSage database is relatively larger than the dataset used for IMCT. All IMCT data come from the data obtained in previous studies, but the data quantity is relatively less. This may be the main reason for the error; however, the calculation principle used for both data sets is the same, based on the Gibbs free energy of the component reaction in the slag. The calculation results indicate that as the TiO_2 content is higher, the calculation results are closer to the experimental results. Summarizing the calculation and experimental results, it can be concluded that the optimal TiO_2 addition amount in the slag is approximately 10% to prevent the oxidation of Al and Ti elements in the alloy during electroslag remelting of the Incoloy 825 alloy.

3 Mass Transfer of Al and Ti Elements During Electroslag Remelting

A kinetic study of the electroslag remelting process was used to predict the changes in the Al and Ti elements in the alloy. In the industrial electroslag process, the slag-metal reaction is more complicated and the thermodynamic applicability is reduced, but analysis is conducted mainly using kinetics. The mass transfer process of Al, Ti, TiO_2, and Al_2O_3 during the electroslag remelting process is shown in Fig.10.

The mass transfer of slag and alloy components occurs in three regions of the slag, i. e. the metal interface at the

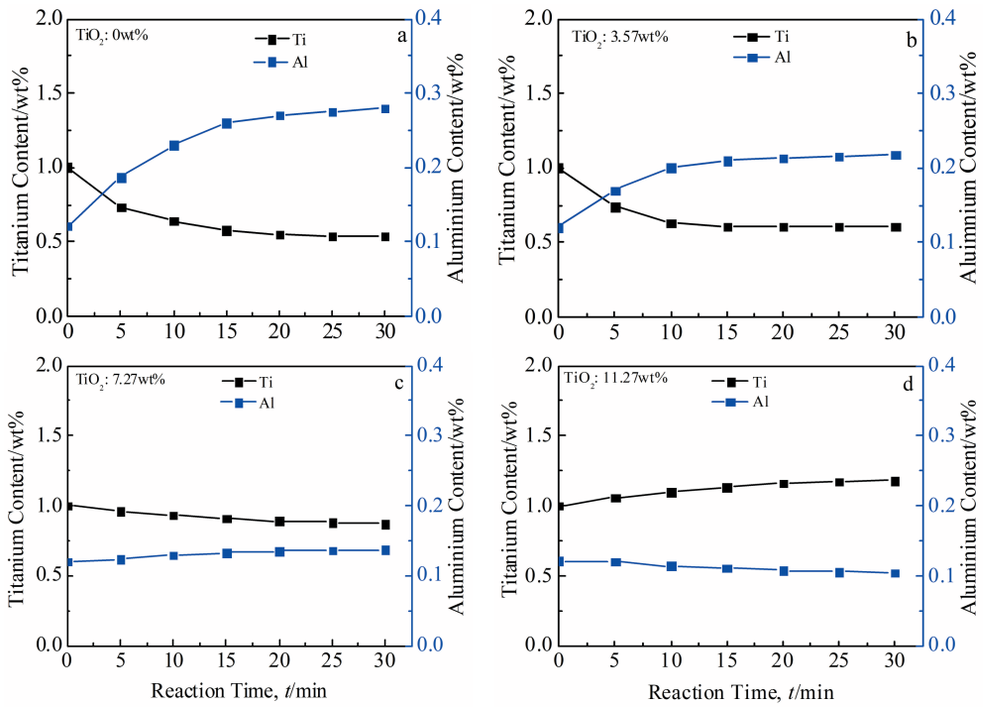

Fig.8 Changes of Al and Ti contents in alloy: (a) TiO_2 content=0wt%, (b) TiO_2 content=3.57wt%, (c) TiO_2 content=7.27wt%, and (d) TiO_2 content=11.27wt%

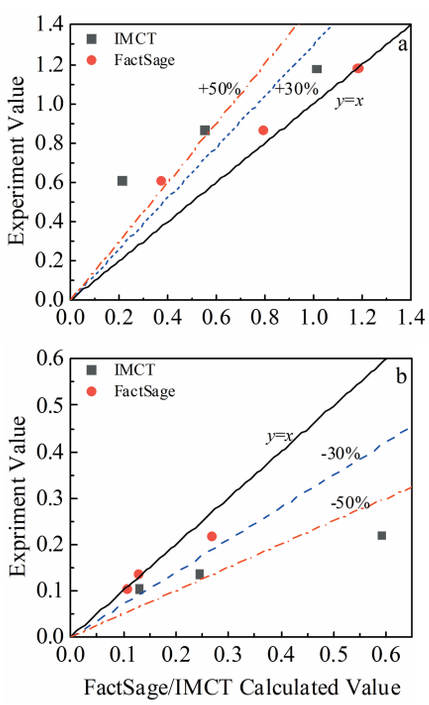

Fig.9 Deviation of Ti (a) and Al (b) between FactSage and IMCT calculated vs. experimental results

electrode tip, the droplet-slag interface in the process of droplet dropping, and the molten metal pool-slag interface. The reaction formulas of Al and Ti in the alloy with Al_2O_3 and TiO_2 in the slag are as shown in Eq.(12) and Eq.(13):

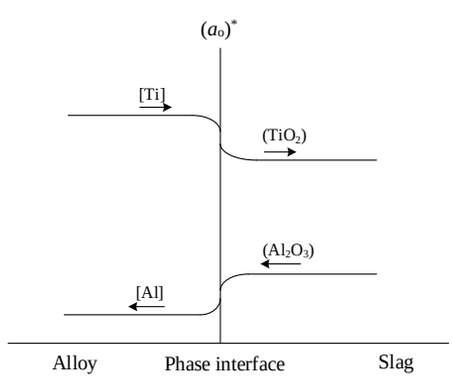

Fig.10 Mass transfer diagram of slag-metal interface

$$[\mathrm{Al}] + 1.5[\mathrm{O}] = (\mathrm{AlO_{1.5}}) \quad (12)$$

$$[\mathrm{Ti}] + 2[\mathrm{O}] = (\mathrm{TiO_2}) \quad (13)$$

The expressions for the equilibrium constants are shown in Eq.(14) and Eq.(15).

$$\lg K_{\mathrm{Al}} = \lg \frac{a^*_{\mathrm{AlO_{1.5}}}}{a^*_{\mathrm{Al}} a^{*\,1.5}_{\mathrm{O}}} = \frac{32000}{T} - 10.29 \quad (14)$$

$$\lg K_{\mathrm{Ti}} = \lg \frac{a^*_{\mathrm{TiO_2}}}{a^*_{\mathrm{Ti}} a^{*\,2}_{\mathrm{O}}} = \frac{34458}{T} - 11.96 \quad (15)$$

According to the film-penetration theory, the diffusion flux of component i can be expressed as Eq.(16):

$$J_i = \frac{k_{i,\mathrm{m}}\rho_{\mathrm{m}}}{100M_i}\left\{[\%i] - [\%i]^*\right\} = \frac{k_{i,\mathrm{s}}\rho_{\mathrm{s}}}{100M_{iO_x}}\left\{(\%iO_x)^* - (\%iO_x)\right\} \quad (16)$$

where J_i is the diffusion flux of i; $k_{i,\mathrm{m}}$and $k_{i,\mathrm{s}}$ are the mass tran-

sfer coefficients of i and iO_x in the alloy and slag, respectively; M_i and M_{iO_x} are the relative atomic masses of i and iO_x, respectively; ρ_m and ρ_s are the densities of the alloy and slag, respectively; $[\%i]^*$ and $(\%iO_x)^*$ are the interfacial concentrations of the components in the molten alloy and slag, respectively.

According to Eq. (16), the interface concentration of element i in the alloy can be expressed as Eq.(17) and Eq.(18):

$$[\%i]^* = \frac{\frac{k_{i,m}\rho_m M_{iO_x}}{k_{i,s}\rho_s M_i}[\%i] + (\%iO_x)}{\frac{k_{i,m}\rho_m M_{iO_x}}{k_{i,s}\rho_s M_i} + B_i a_O^{*x}} \quad (17)$$

$$B_i = \frac{(\%iO_x)^*}{[\%i]^* a_O^{*x}} = \frac{M_{iO_x} f_i K_M \left\{\frac{(\%CaF_2)}{M_{CaF_2}} + \sum\frac{(\%iO_x)}{M_{iO_x}}\right\}}{\gamma_{iO_x}} \quad (18)$$

where a_O^* is the interface oxygen activity and K_M is the equilibrium constant. The activity coefficient of the components in the alloy, f_M, and the activity coefficient of component iO_x in the slag, γ_{iO_x}, are calculated using Eq. (19) and Eq.(20), respectively:

$$\lg f_i = \sum\left(e_i^j[\%j] + r_i^j[\%j]^2\right) \quad (19)$$

$$\gamma_{iO_x} = \frac{a_{iO_x}}{(\%iO_x)} \quad (20)$$

where e_i^j and r_i^j are the first-order and second-order interaction parameters in the alloy, respectively. The first-order interaction coefficients are listed in Table 1. The currently available second-order interaction coefficients are summarized as: $r_{Al}^{C} = -0.004$, $r_{Al}^{Al} = (-0.0011 + 0.17/T)$, $r_{Al}^{Si} = -0.0006$, $r_{Al}^{Ni} = 0.000164$, $r_{Si}^{Si} = (-0.0055 + 6.5/T)$, $r_{Si}^{Cr} = 0.00043$, $r_{Ti}^{Ti} = -0.001$, $r_{Ti}^{Ni} = 0.0005$[37]. The activity of the components in the slag is represented by a_{iO_x}.

$$-\frac{d[\%Al]}{dt} = \left(\frac{A}{W_m}k_{Al}\right)\left\{[\%Al] - \frac{(\%AlO_{1.5})}{B_{Al}a_O^{*1.5}}\right\} \quad (21)$$

$$-\frac{d[\%Ti]}{dt} = \left(\frac{A}{W_m}k_{Ti}\right)\left\{[\%Ti] - \frac{(\%TiO_2)}{B_{Ti}a_O^{*2}}\right\} \quad (22)$$

$$-\frac{d[\%O]}{dt} = \left(\frac{A}{W_m}k_O\right)\left\{[\%O] - \frac{a_O^*}{f_O}\right\} \quad (23)$$

$$\frac{1}{k_i} = \frac{1}{k_{i,m}\rho_m} + \frac{M_{iO_x}}{B_i k_{i,s}\rho_s M_i a_O^{*x}} \quad (24)$$

where W_m is the mass of molten steel and k_i is the comprehensive mass transfer coefficient. The interfacial oxygen activity can be determined according to the mass conservation of elements at the interface, as shown in Eq.(25).

$$\frac{1.5}{M_{Al}}\cdot\frac{d[\%Al]}{dt} + \frac{2}{M_{Ti}}\cdot\frac{d[\%Ti]}{dt} - \frac{1}{M_O}\frac{d[\%O]}{dt} = 0 \quad (25)$$

According to Eq.(21~25), mathematical expressions for the change in Al and Ti contents in the alloy can be obtained, and expressed as Eq.(26) and Eq.(27):

$$[\%Al] = EXP\left(-\frac{A}{W_m}k_{Al}t\right)\left\{[\%Al] - \frac{(\%AlO_{1.5})}{B_{Al}a_O^{*1.5}}\right\} + \frac{(\%AlO_{1.5})}{B_{Al}a_O^{*1.5}} \quad (26)$$

$$[\%Ti] = EXP\left(-\frac{A}{W_m}k_{Ti}t\right)\times\left\{[\%Ti] - \frac{(\%TiO_2)}{B_{Ti}a_O^{*2}}\right\} + \frac{(\%TiO_2)}{B_{Ti}a_O^{*2}} \quad (27)$$

According to the conservation of mass, the contents of Al_2O_3 and TiO_2 in the slag can be obtained. The mass transfer coefficients for different regions are obtained using Eq. (28) and Eq.(29):

$$k_{i,m} = 2\frac{\sqrt{D_i}}{\sqrt{\pi t}} \quad (28)$$

$$k_{i,s} = 2\frac{\sqrt{D_{iO_x}}}{\sqrt{\pi t}} \quad (29)$$

where D_i and D_{iO_x} are the diffusion coefficients of the components in the alloy and slag, respectively, and t is the slag-metal reaction time at different reaction regions. The values of the diffusion coefficients are listed in Table 5.

The mathematical expressions for calculating the mass transfer resistance of the Al and Ti elements in the alloy and Al_2O_3 and TiO_2 in the slag are shown in Table 6. According to Table 6, the rate-determining step during the process of electroslag remelting can be obtained.

According to the above kinetic model results, the change of Al and Ti elements in the ingot during the electroslag remelting process can be predicted. This reduces the experiment cost, and clarifies the control factors of Al and Ti content in the reaction process, as well as the rate-determining step in the slag-metal reaction process. It can provide theoretical guidance for improving the technology conditions of electroslag remelting.

Fraser et al[39, 40] proposed a kinetic model in the electroslag remelting process using the film-penetration theory to study the mass transfer behavior between the two systems, Mn + MnO and Fe + FeO. The model is relatively simple. The mass

Table 5 Relevant component diffusion coefficients of alloy and slag[38]

Temperature/K	D_{Al}/× 10^{-5} $cm^2\cdot s^{-1}$	D_{Ti}/× 10^{-5} $cm^2\cdot s^{-1}$	D_O/× 10^{-5} $cm^2\cdot s^{-1}$	$D_{Al_2O_3}$/×10^{-6} $cm^2\cdot s^{-1}$	D_{TiO_2}/×10^{-5} $cm^2\cdot s^{-1}$
1750	1.5	1.5	1.5	7.1	2.7
1773	2.7	2.7	2.7	7.8	3.0
1798	4.4	4.4	4.4	9.0	3.5
1923	57	57	57	35	6.0
1938	77	77	77	42	7.2
1950	92	92	92	50	8.0

Table 6 Mass transfer resistance of components in alloy and slag

Al, Ti	Al_2O_3	TiO_2
$\frac{1}{\rho_m \cdot k_{i,m}}$	$\frac{M_{AlO_{1.5}}}{B_{Al} M_{Al} \rho_s k_s a_O^{*\,1.5}}$	$\frac{M_{TiO_2}}{B_{Ti} M_{Ti} \rho_s k_s a_O^{*\,2}}$

transfer process of the electroslag remelting process was analyzed in detail, and the mass transfer coefficient and mass transfer time were derived. Based on a large number of experiments, the feasibility and rationality of the model were verified. Schwerdtfeger et al[41] obtained a mass transfer model

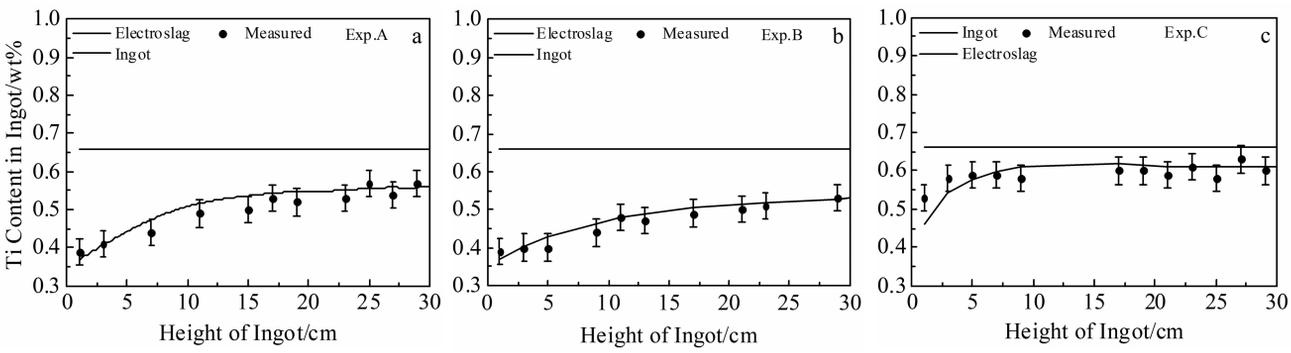

Fig.11 Variation of Ti content in consumable electrodes and electroslag ingots[38,44]: (a) Exp. A, (b) Exp. B, and (c) Exp. C

of the Al+Al_2O_3, Ti+TiO_2, and Fe+FeO systems in the electroslag process based on the results of Fraser's research, and predicted the Al, Ti, and Al_2O_3 and TiO_2 contents in the steel in the electroslag remelting process. The composition change of the ingot is in good agreement with the experimental results. Wei et al[42,43] optimized the model of Fraser, and proposed a kinetic model of the heterogeneous reaction in the electroslag process. The optimized model used a CaF_2-Al_2O_3 (argon atmosphere) and a CaF_2-CaO-Al_2O_3 (air atmosphere) slag system to subject SAE 1020 steel to electroslag remelting on a 1t UBC 250 kVA electroslag furnace. The results show that the burning loss of Si in the steel during the electroslag remelting process under an argon atmosphere is significantly improved, and the burning loss of Al, Si, and Mn in the alloy is mainly due to the strong oxidation of FeO. The model also explains that the influence of CaO in the slag on the activity of SiO_2 and Al_2O_3 is the key to control Si/Al in the electroslag ingot. Hou et al[38,44] proposed a kinetic model for mass transfer in Al + Al_2O_3, Ti + TiO_2, Si + SiO_2, and Fe + FeO systems and tested the model with CaF_2-CaO-Al_2O_3-SiO_2-TiO_2-MgO slag and 1Cr21Ni5Ti in electroslag remelting experiments on a 50 kg electroslag furnace. The model calculation results are in good agreement with the experimental results. The Al, Ti, and Si in the steel and Al_2O_3, TiO_2, and SiO_2 in the slag, as calculated by the model, accurately predicted the variation in the composition of the electroslag ingot. The model also identified the rate-determining steps of the reaction: mass transfer of alumina through the molten steel, silica through the slag, and titanium on both the metal and slag sides. In addition, it is found that the addition of 200 g TiO_2 during the initial heating stage of electroslag remelting can significantly inhibit the loss of Ti.

Fig. 11 illustrates that even under the optimal process conditions and slag system, Ti loss inevitably occurs in the ingot. This may be due to the complex environment in the actual electroslag process and the difficulty of imposing stable controls in the process. In the initial heating stage, particularly, the fluctuation range of metal elements is relatively large. Therefore, it is necessary to use the kinetic method in the electroslag remelting process to further explore improvements in process conditions. Our current kinetic model considers relatively few actual factors, and more accurate models are needed for the future development processes. However, our model more closely represents the actual process, which not only helps to have a clearer and deeper understanding of the entire electroslag remelting process, but also further optimizes the process parameters and slag system ratio, and more accurately controls the Al and Ti content.

4 Conclusions

1) Based on previous research, our study summarizes the thermodynamic and kinetic methods to control the Al and Ti content in the process of electroslag remelting. The results of the thermodynamic calculations indicate that an increase in temperature increases the oxidation of Ti and inhibits the oxidation of Al.

2) The increase in CaO and Al_2O_3 content in the slag increases the oxidation of Ti; however, when the Al_2O_3 content is greater than 15%, the oxidation of Ti in the alloy becomes weaker. The higher content of CaO and Al_2O_3 in the low-fluorine slag system requires addition of more TiO_2 to inhibit the oxidation of Ti in the alloy. Increasing the TiO_2 content significantly inhibits Ti oxidation, but different alloys require different amounts of TiO_2.

3) The FactSage calculation result has a small deviation from the slag-metal equilibrium experiment result, while the IMCT calculation result is slightly larger than the experimental result. As the TiO_2 content in the slag increases, the calculation results are closer to the experimental results.

Based on the film-penetration theory, a kinetic model is proposed for the process of electroslag remelting, and the mathematical expressions for the change in the Al and Ti element content and the rate-determining step in the process of electroslag remelting can be obtained.

References

1 Ju J T, Ji G H, Tang C M *et al*. *Steel Research International*[J], 2020, 91(9): 2 000 111

2 Sun N, Wen C, Liu Z L *et al*. *Rare Metal Materials and Engineering* [J], 2018, 47(3): 860

3 Navid Sayyar, Morteza Shamanian, Behzad Niroumand. *Journal of Materials Processing Technology*[J], 2018, 262: 562

4 Guo J, Geng Z Y, Dong J X *et al*. *Rare Metal Materials and Engineering*[J], 2012, 41(11): 1929

5 Ju J T, Yang K S, Ji G H *et al*. *Rare Metal Materials and Engineering* [J], 2020, 49(11): 3676

6 Chen S C, Wang X P, Ning T X *et al*. *Special Steel*[J], 2017, 38 (6): 49

7 Li S. *Journal of Iron and Steel Research* [J], 2011, 23(S2): 282

8 Xue Z X, Zheng Y X, Jiang F *et al*. *Special Steel*[J], 2016, 37(4): 37

9 Duan S C, Guo H J, Shi X *et al. Chinese Journal of Engineering* [J], 2018, 40(S1): 53

10 Hou D, Jiang Z H, Dong Y W *et al*. *Metallurgical and Materials Transactions B*[J], 2017, 48: 1885

11 Li S J, Cheng G G, Miao Z Q *et al*. *ISIJ International*[J], 2017, 57(12): 2148

12 Hou D, Jiang Z H, Qu T P *et al*. *Journal of Iron and Steel Research International*[J], 2019, 26: 20

13 Duan S C, Shi X, Wang F *et al. Journal of Materials Research and Technology*[J], 2019, 8(3): 2508

14 Chen C X, Wang Y, Fu J *et al. Acta Metallurgica Sinica*[J], 1981, 17(1): 50

15 Yin B, Li W M, Wu S P *et al*. *Iron and Steel*[J], 2019, 54(5): 86

16 Hou D, Liu F B, Qu T P *et al*. *ISIJ International*[J], 2018, 58(5): 876

17 Deng P H, Zhou L X, Pang M X *et al. Special Steel*[J], 2015, 36(1): 38

18 Hou D, Wang D Y, Qu T P *et al*. *Metallurgical and Materials Transactions B*[J], 2019, 50: 3088

19 Pateisky G, Biele H, Fleischer H J. *Journal of Vacuum Science and Technology*[J], 1972, 9: 1318

20 Suzuki K, Ban-Ya S, Hino M. *ISIJ International*[J], 2002, 42(2): 146

21 Yoshikawa T, Morita K. *Metallurgical and Materials Transactions B*[J], 2007, 38(4): 671

22 Pak J J, Jeong Y S, Tae S J *et al*. *Metallurgical and Materials Transactions B*[J], 2005, 36: 489

23 Jerzak W, Kalicka Z. *Archives of Metallurgy and Materials*[J], 2012, 57(2): 449

24 Yang X M, Jiao J S, Ding R C *et al*. *ISIJ International*[J], 2009, 49(12): 1828

25 Yang X M, Shi C B, Zhang M et al. *Metallurgical and Materials Transactions B*[J], 2011, 42: 1150

26 Yang X M, Shi C B, Zhang M *et al*. *Metallurgical and Materials Transactions B*[J], 2011, 42: 951

27 Li J X, Zhang J. *Journal of University of Science and Technology Beijing*[J], 2000, 4: 316

28 Yang X M, Shi C B, Zhang M *et al*. *Steel Research International* [J], 2012, 83(3): 244

29 Duan S, Shi X, Mao M *et al*. *Scientific Reports*[J], 2018, 8: 5232

30 Hou D, Dong Y W, Jiang Z H *et al*. *Journal of Northeastern University (Natural Science)*[J], 2015, 36(11): 1591

31 Yang J G, Park J H. *Metallurgical and Materials Transactions B* [J], 2017, 48: 2147

32 Jiang Z H, Hou D, Dong Y W *et al*. *Metallurgical and Materials Transactions B*[J], 2016, 47: 1465

33 Hou D, Jiang Z H, Dong Y W *et al*. *Ironmaking & Steelmaking* [J], 2016, 43(7): 1

34 Duan S C, Shi X, Wang F *et al*. *Metallurgical and Materials Transactions B*[J], 2019, 50: 3055

35 Shi C B, Zheng D L, Shin S H *et al*. *International Journal of Minerals, Metallurgy and Materials*[J], 2017, 24(1): 18

36 Ju J T, An J L, Shi C B *et al*. *Rare Metal Materials and Engineering*[J], 2020, 49(1): 233

37 Karasev A, Suito H. *Metallurgical and Materials Transactions B* [J], 1999, 30: 249

38 Hou D, Jiang Z H, Dong Y W *et al*. *ISIJ International*[J], 2017, 57(8): 1400

39 Fraser M E, Mitchell A. *Ironmaking & Steelmaking*[J], 1976, 3(5): 279

40 Fraser M E, Mitchell A. *Ironmaking & Steelmaking*[J], 1976, 3(5): 288

41 Schwerdtfeger K, Wepner W, Pateisky G. *Ironmaking & Steelmaking*[J], 1978, 5(3): 135

42 Wei J H, Mitchell A. *Acta Metallurgica Sinica*[J], 1984, 20(5): 387

43 Wei J H, Mitchell A. *Acta Metallurgica Sinica*[J], 1984, 20(5): 406

44 Hou D, Jiang Z H, Dong Y W *et al*. *ISIJ International*[J], 2017, 57(8): 1410

高温镍基合金电渣重熔过程中的Al、Ti成分控制

巨建涛[1,2]，朱智洪[1,2]，杨康帅[1,2]，棘广恒[1,2]，安家良[1,2]，史成斌[3]

(1. 西安建筑科技大学 冶金工程学院，陕西 西安 710055)

(2. 陕西省冶金工程技术研究中心，陕西 西安 710055)

(3. 北京科技大学 冶金新技术国家重点实验室，北京 100083)

摘　要：电渣重熔过程中Al和Ti的氧化导致电渣锭轴向成分不均匀，从而对电渣锭的耐腐蚀性能和力学性能产生不利影响。为了控制电渣铸锭中Al和Ti含量的均匀性，需要明确高温电渣重熔过程中Al和Ti含量的变化，并通过优化渣体系比例和冶炼条件来减少合金中Al和Ti的氧化。在现有文献的基础上，以CaF_2-CaO-Al_2O_3-MgO-TiO_2这一低氟渣系和Incoloy825合金为例，综述了电渣重熔过程中Al和Ti元素控制的研究现状。应用离子与分子共存理论（IMCT），结合FactSage软件，总结了渣的热力学和动力学研究方法。讨论了温度和渣成分对合金中平衡Al、Ti含量的影响。基于膜渗透理论，提出了预测合金中Al和Ti含量的动力学模型，得到了电渣过程中Al和Ti含量随时间变化的数学方程式以及渣-金属反应速率的限制方法。确定电渣重熔Incoloy825合金时TiO_2的最佳添加量约为10%。用IMCT和FactSage对渣-金平衡实验结果进行了比较和分析。FactSage计算结果比IMCT计算结果更准确。TiO_2含量越高，计算结果与实验结果之间的偏差越小。

关键词：电渣重熔；Al、Ti含量；热力学；离子分子共存理论；动力学

作者简介：巨建涛，男，1973年生，博士，教授级高级工程师，西安建筑科技大学冶金工程学院，陕西 西安 710055，电话：029-82205114，E-mail：jujiantao_0033@163.com